Intrinsic GTPase activity of K-RAS monitored by native mass spectrometry

Zahra Moghadamchargari[1], Jamison Huddleston[1], Mehdi Shirzadeh[1], Xueyun Zheng[1], David E. Clemmer[2], Frank M. Raushel[1], David H. Russell[1], and Arthur Laganowsky[1,*]

[1] Department of Chemistry, Texas A&M University, College Station, Texas.

[2]Department of Chemistry, Indiana University, Bloomington, Indiana.

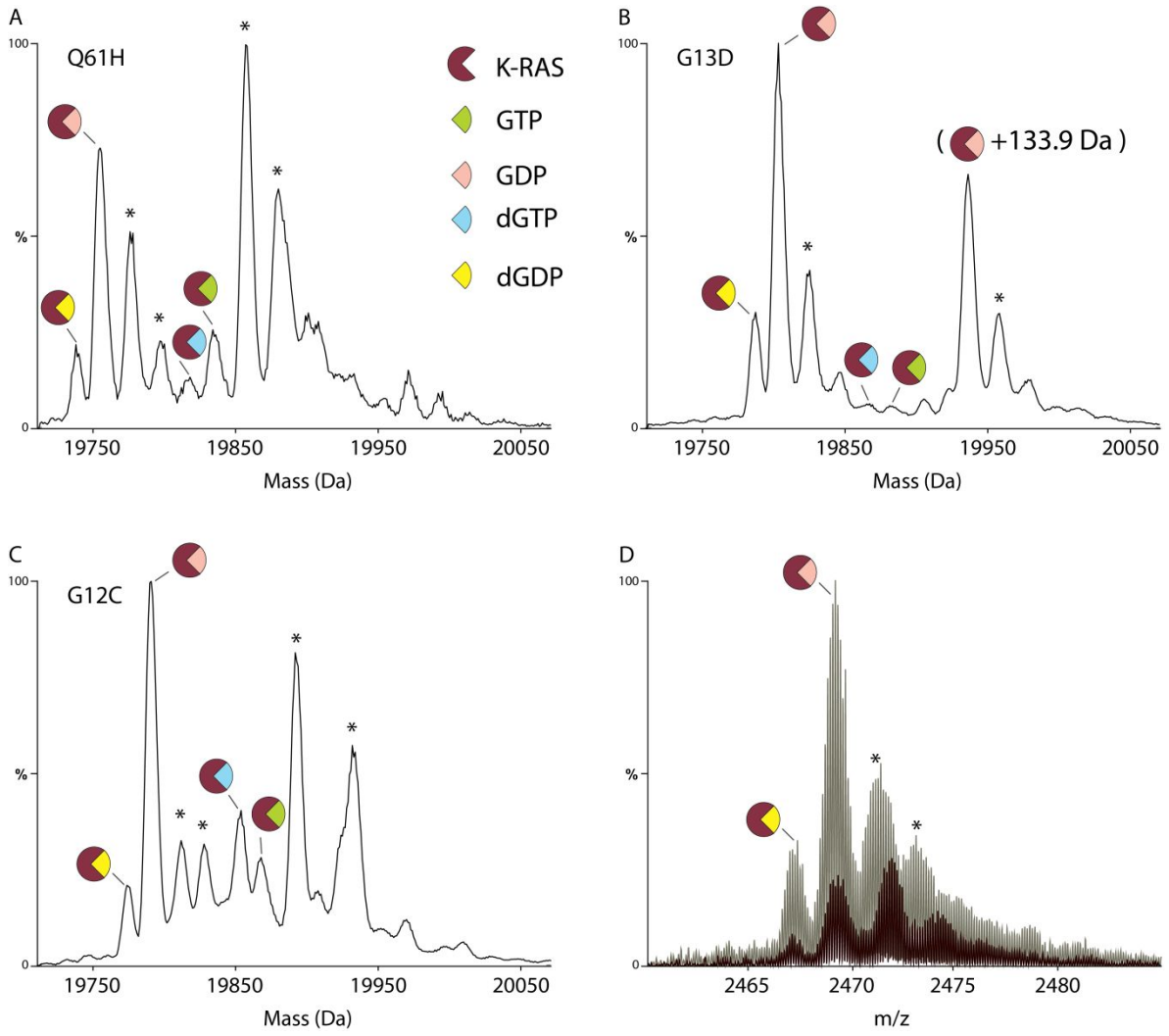

Figure S1. Deconvolution of native mass spectra for oncogenic K-RAS mutants (A) Q61H, (B) G13D and (C) G12C reveal binding of 2'-deoxy and 2'-hydroxy forms of GDP and GTP. (D) Overlay of native mass spectra of K-RAS (8+) as isolated (gray) and with magnesium acetate added to the spray solution (maroon). Asterisk denotes bound sodium or magnesium adducts.

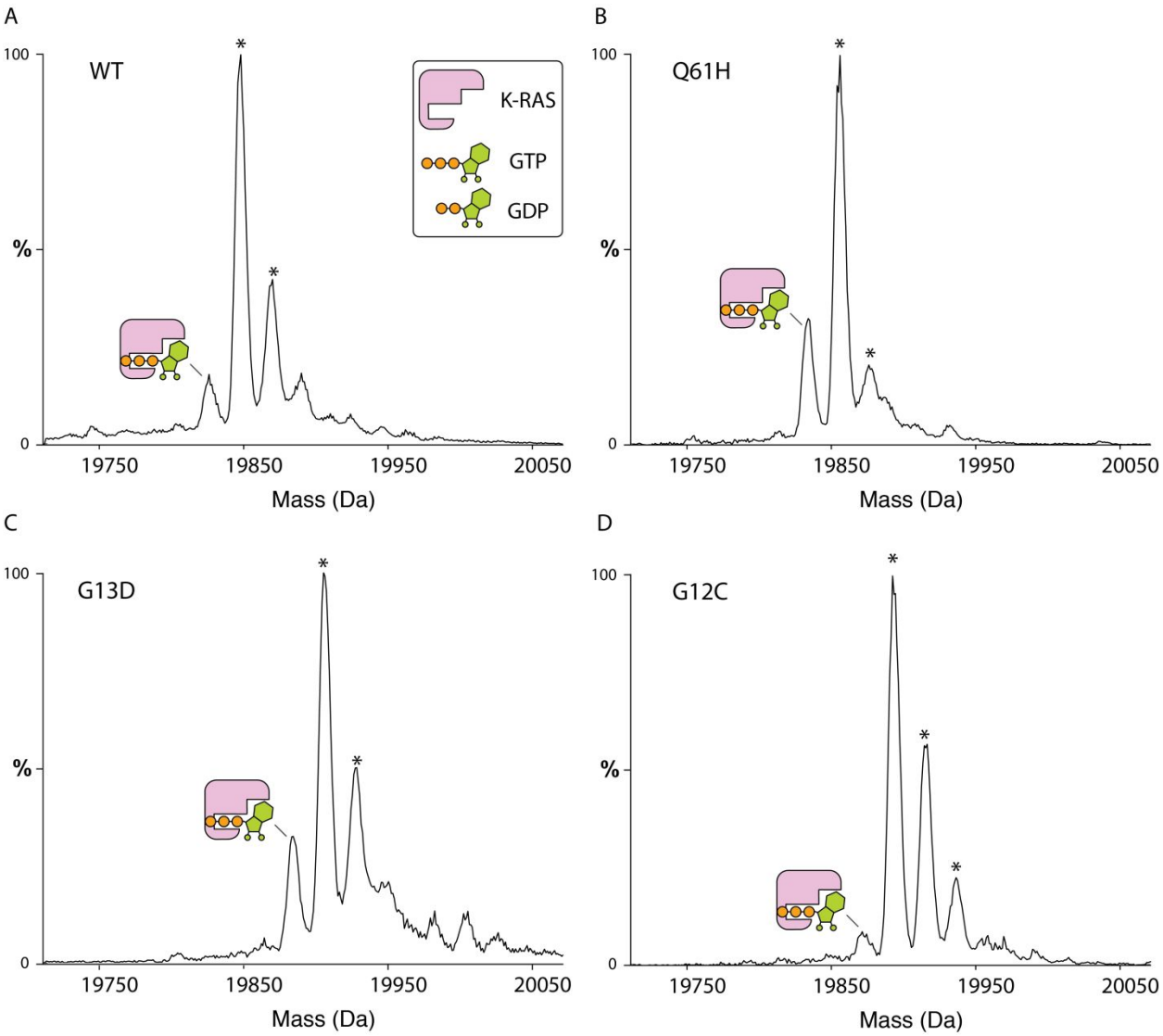

Figure S2. Deconvolution of native mass spectra for K-RAS (A) WT, (B) Q61H, (C) G13D and (D) G12C loaded with GTP. Asterisk represents bound sodium or magnesium adducts.

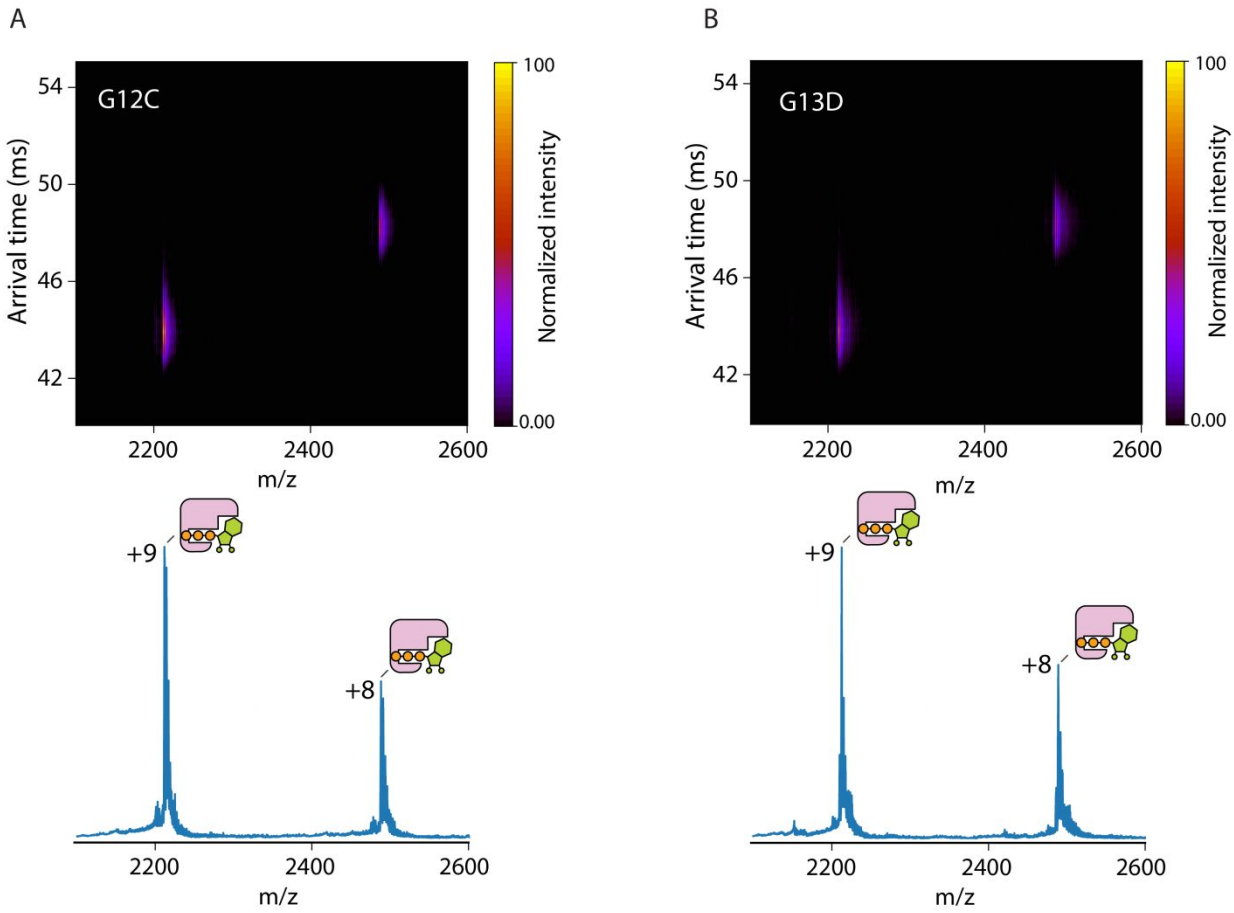

Figure S3. 2D Ion mobility mass spectra of K-RAS (A) G12C and (B) G13D. All mutants were loaded with GTP.

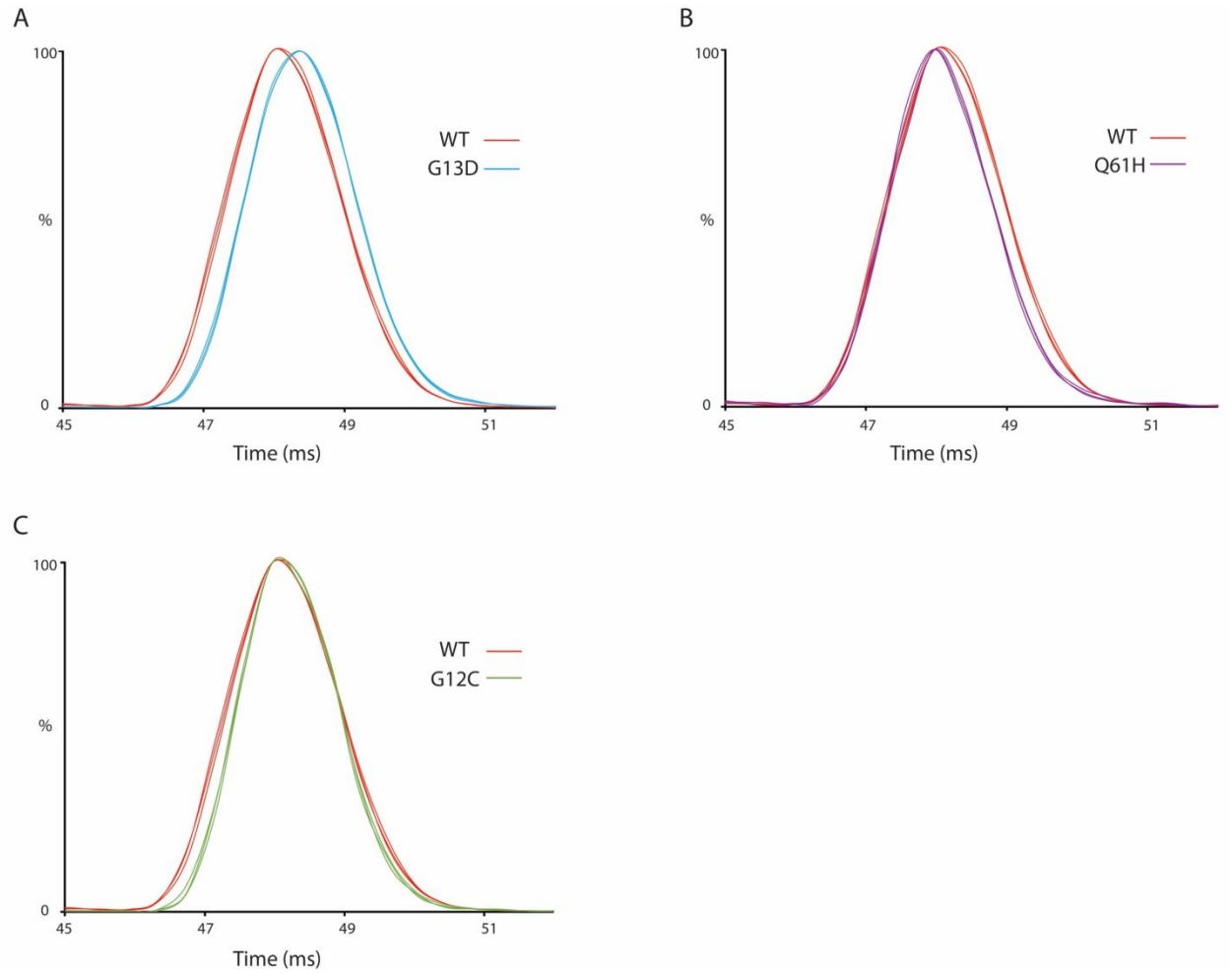

Figure S4. Comparison of arrival time distributions (ATD) of K-RAS and mutants bound to GTP. ATD are shown for the 8^{+} charge state and repeated measurements overlaid.

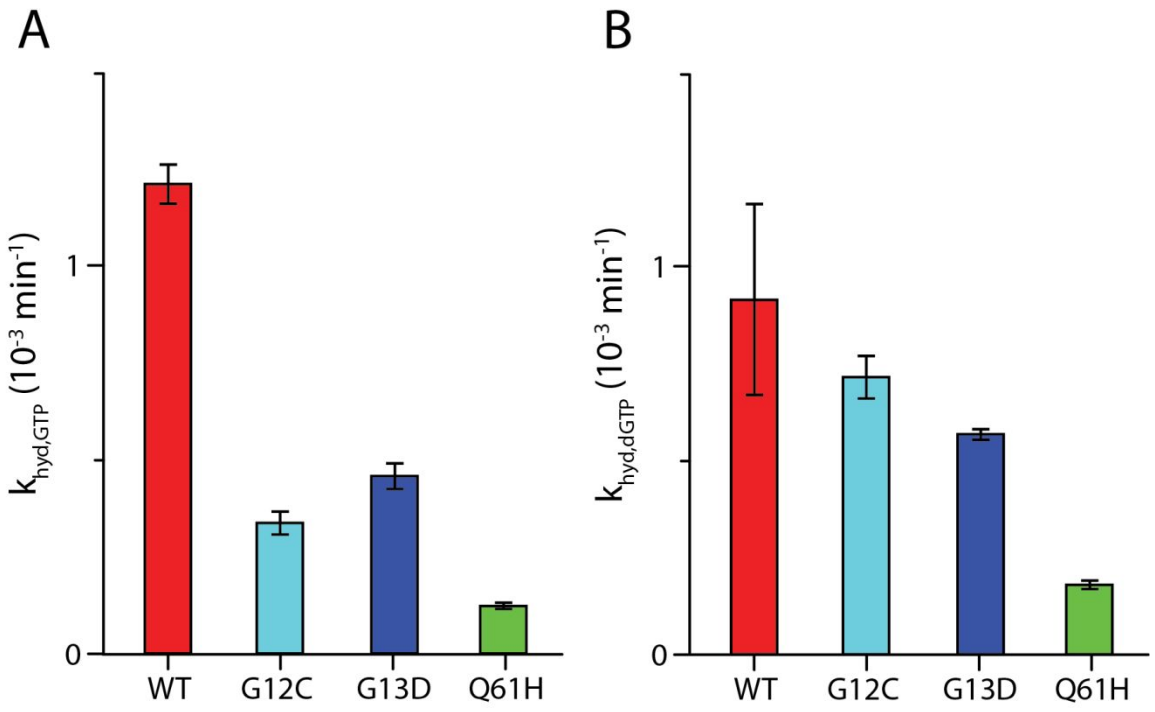

Figure S5. The rate of intrinsic GTP hydrolysis for K-RAS and mutants loaded with (A) GTP or (B) dGTP. Reported are the mean and standard deviation (n = 3).

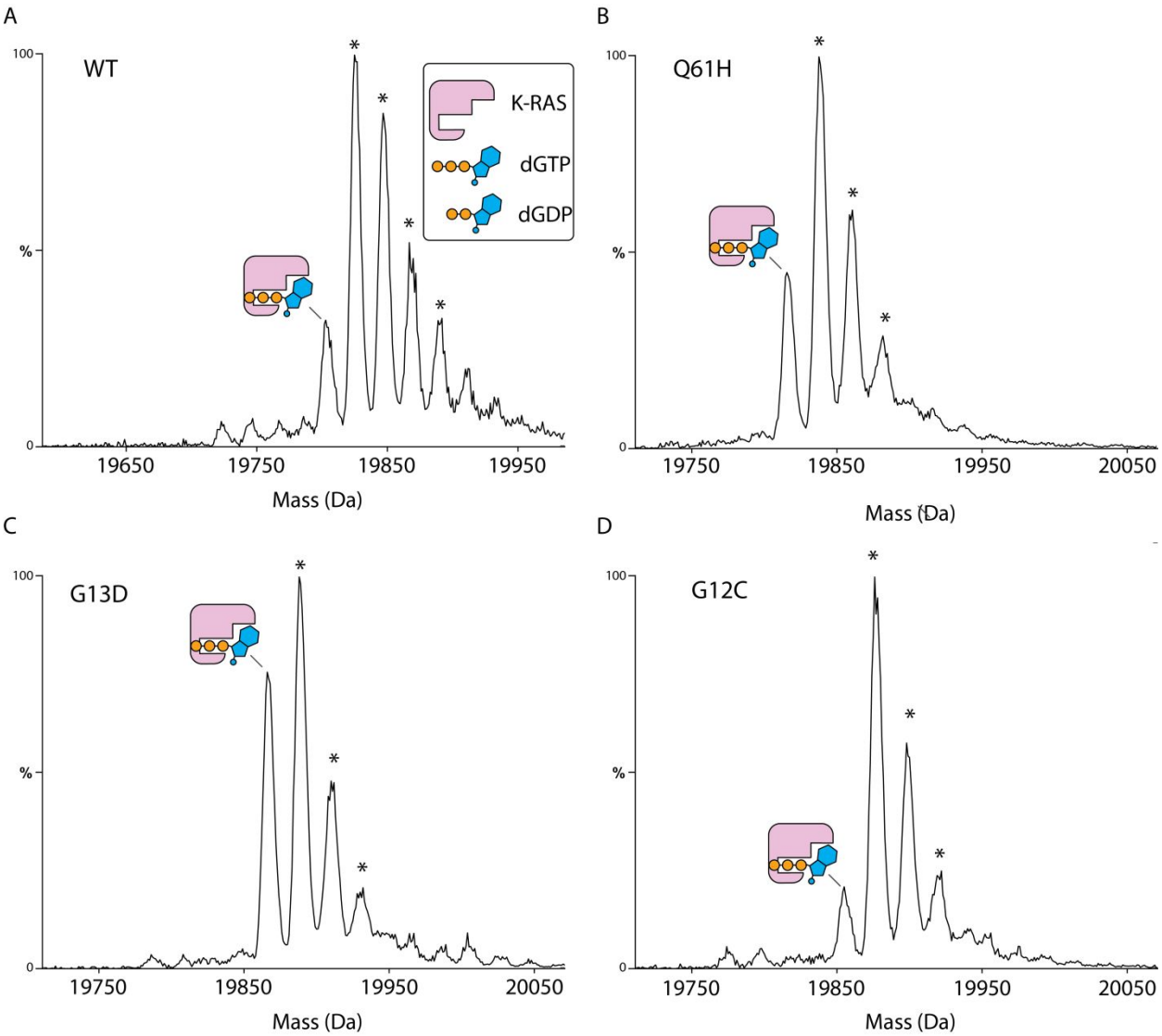

Figure S6. Deconvolution of native mass spectra for K-RAS (A) WT, (B) Q61H, (C) G13D and (D) G12C loaded with dGTP. Asterisk represents sodium or magnesium bound adducts.

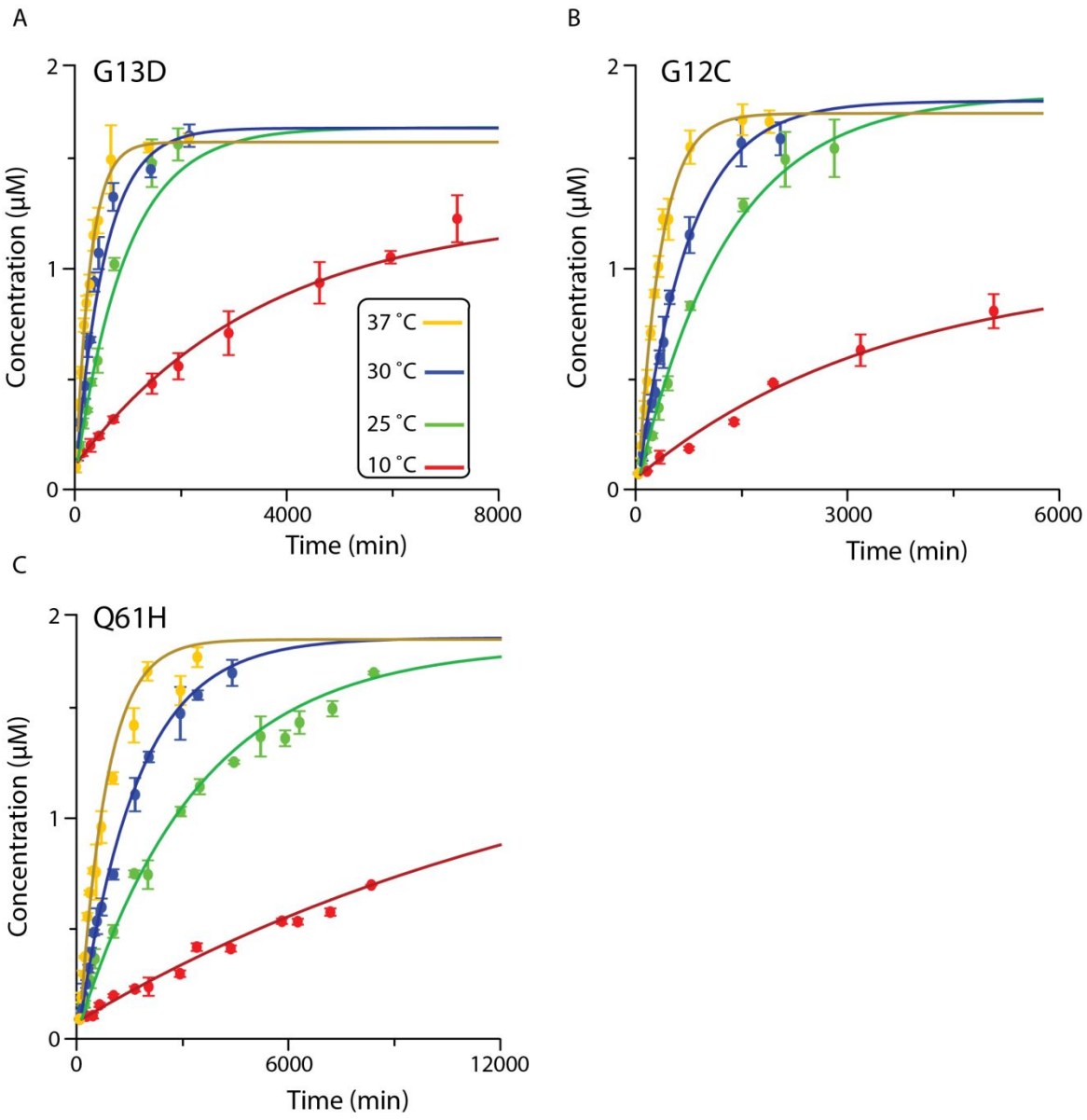

Figure S7. The temperature dependence of intrinsic GTP hydrolysis of K-RAS (A) G13D, (B) G12C and (C) Q61H.

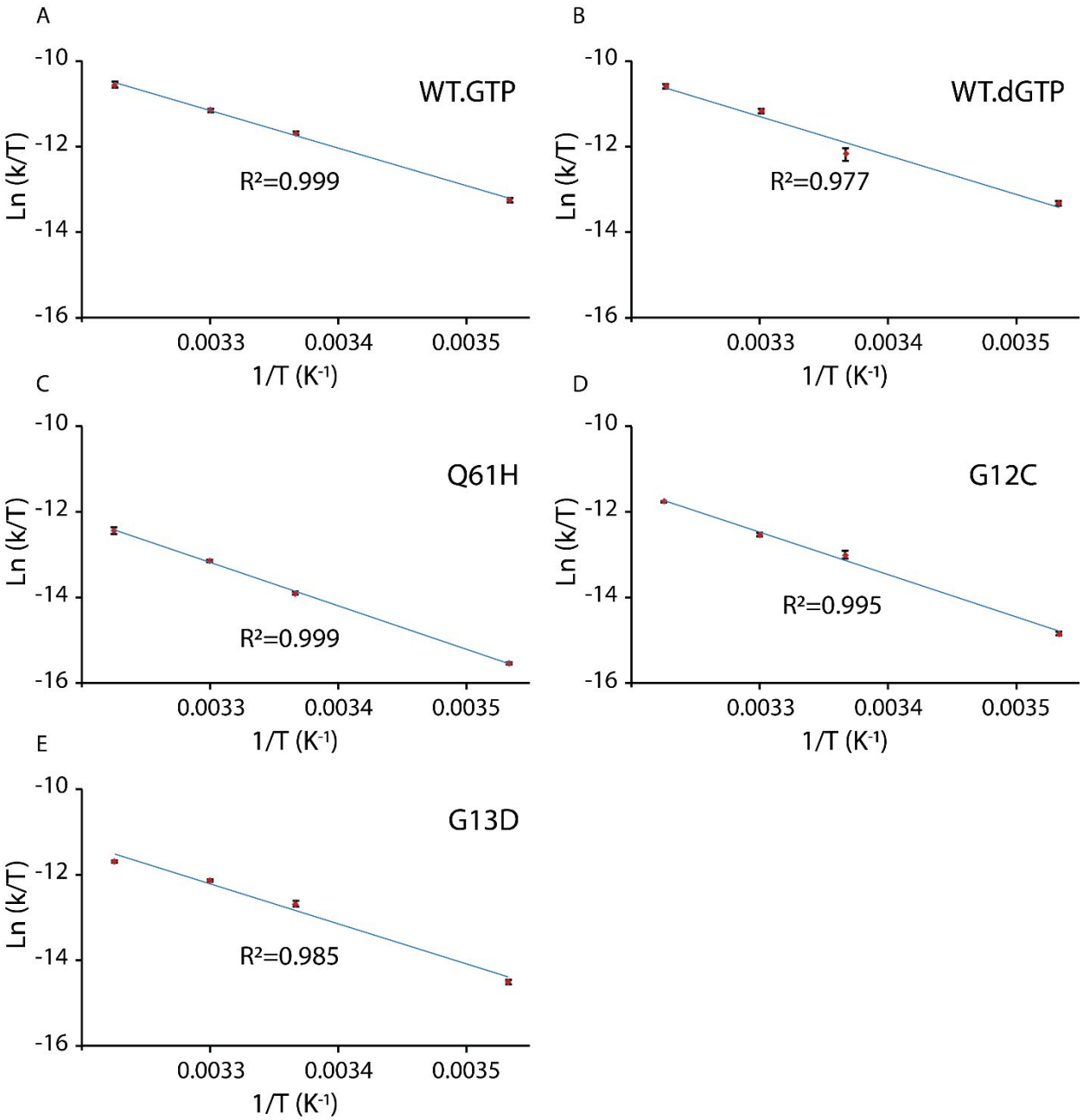

Figure S8. Eyring plots generated for K-RAS (A) WT•GTP, (B) WT•dGTP, (C) Q61H•GTP, (D) G12C•GTP and (E) G13D•GTP. All data shown are the mean and standard deviation (n=3).

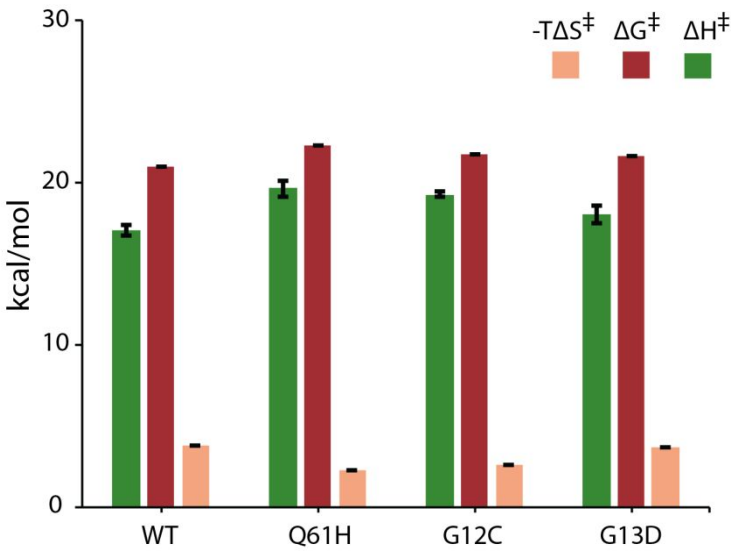

Fig S9. Enthalpy ($\Delta H^{\ddagger}$), entropy ($\Delta S^{\ddagger}$) and change in Gibbs free energy ($\Delta G^{\ddagger}$) of activation determined by Eyring analysis (T=298 K). Reported are the mean and standard deviation (n = 3).

Table S1. The optimized parameters used for quantitative analysis of intrinsic hydrolysis using Q Exactive EMR.

m/z range	2000-3000
Resolution	140000
In-source collision energy dissociation (V)	10
Source temperature (°C)	100
Capillary voltage (KV)	1.6
Source DC offset (V)	25
Injection flatapole lens(V)	15
Inter flatapole DC (V)	10
Bent flatapole DC (V)	6
Transfer multipole DC (V)	2
Pressure (mbar)	3.4×10^{-10}

Table S2. NanoESI condition and front funnel settings for the 20,000 m/z extended mass range ion mode (Agilent 6560).

Capillary voltage (V)	1000-2000
Drying gas temperature (℃)	200
Drying gas flow (L/min)	1.5
Fragmentor (V)	400
High Pressure funnel delta (V)	150
High Pressure Funnel RF (V)	200
Trap funnel delta (V)	180
Trap funnel RF (V)	200
Trap Funnel Exit (V)	10

Table S3. Drift Tube Settings for Stepped Field Experiments in Positive Ion Mode

Time Sequence	Time (min)	Drift Tube Entrance (V)	Drift Tube Exit (V)	Rear Funnel Entrance (V)	Rear Funnel Exit (V)
1	0.0 – 0.5	1074	224	217.5	45
2	0.5 – 1.0	1174	224	217.5	45
3	1.0 – 1.5	1274	224	217.5	45
4	1.5 – 2.0	1374	224	217.5	45
5	2.0 – 2.5	1474	224	217.5	45
6	2.5 – 3.0	1574	224	217.5	45
7	3.0 – 3.5	1674	224	217.5	45

Table S4. Theoretical and measured monoisotopic masses for 2'-deoxy and 2'-hydroxy forms of GDP and GTP bound to K-RAS WT and mutants. The measured monoisotopic mass is calculated by deconvolution the native mass spectra using Thermo protein deconvolution software.

Protein	Species	Measured monoisotopic mass (Da)	Theoretical monoisotopic mass (Da)	Average mass (Da)	ppm
WT	dGDP	19717.69	19717.67	19729.12	0.938
	GDP	19733.71	19733.67	19745.04	2.11
	dGTP	19796.60	19796.63	19797.92	1.58
	GTP	19810.56	19812.63	19820.96	104.57
G12C	dGDP	19762.93	19763.64	19775.04	35.86
	GDP	19778.96	19779.64	19791.04	34.40
	dGTP	19841.87	19842.60	19853.92	37.09
	GTP	19855.88	19858.60	19868.00	137.31
G13D	dGDP	19775.69	19776.68	19786.72	50.04
	GDP	19791.71	19792.68	19803.68	48.95
	dGTP	19854.61	19855.64	19865.60	51.98
	GTP	19873.57	19871.64	19881.60	97.42
Q61H	dGDP	19726.60	19727.67	19737.68	54.44
	GDP	19742.63	19743.67	19753.68	52.63
	dGTP	19805.56	19806.63	19817.68	54.27
	GTP	19821.58	19822.63	19834.64	53.12

Table S5. Collision cross section (CCS) values for the 8+ charge state of K-RAS and mutants bound to dGTP. Reported are the mean and standard deviation for the centroid CCS values (n = 3).

Protein	CCS (Å^2)
K-RAS	1937.6 ± 10.9
K-RAS^{G12C}	1936.2 ± 7.4
K-RAS^{G13D}	1941.0 ± 5.2
K-RAS^{Q61H}	1921.9 ± 3.4

Table S6. The CCS calculated using IMPACT.

Protein	**PDB code**	**CCS (Å^2)**
KRAS^{WT}.GTP	5VQ2	1909.4 ± 6.3
KRAS^{Q61H}.GTP	3GFT	1924.7 ± 7.9
KRAS^{WT}.GDP	4OBE	1948.3 ± 5.1
KRAS^{WT}.GDP	4LPK	1822.4 ± 3.9
KRAS^{G12C}.GDP	4L8G	1819.4 ± 6
KRAS^{G12C}.GDP	4LDJ	2006.9 ± 8
KRAS^{G13D}.GDP	4TQA	1952.9 ± 7.2

Table S7. Thermodynamics of intrinsic GTPase activity for K-RAS loaded with dGTP.

Protein	**$\Delta S^{\ddagger}$ (kcal/mol)**	**$\Delta H^{\ddagger}$ (kcal/mol)**	**$\Delta G^{\ddagger}$ (kcal/mol)**
KRAS^{WT}.dGTP	-0.0122 ± 0.0009	17.4 ± 0.3	21.06 ± 0.04